Influence of rigid inclusions on the bending elasticity of a lipid membrane

Miha Fošnarič* and Aleš Iglič
Laboratory of Physics, Faculty of Electrical Engineering, University of Ljubljana, Tržaška 25, SI-1000 Ljubljana, Slovenia

Sylvio May†
Department of Physics, North Dakota State University, P.O. Box 5566, Fargo, North Dakota 58105-5566, USA
(Received 8 August 2006; published 7 November 2006)

We model the influence of rigid inclusions on the curvature elasticity of a lipid membrane. Our focus is on conelike transmembrane inclusions that are able to induce long-range deformations in the host bilayer membrane. The elastic properties of the membrane are described in terms of curvature and tilt elasticity. The latter adds an additional degree of freedom that allows the membrane to accommodate an inclusion not only through a curvature deformation but also via changes in lipid tilt. Using a (mean-field level) cell model for homogeneously distributed inclusions in a small membrane segment of prescribed (mesoscopic-scale) spherical shape, we calculate the optimal microscopic-scale deviation of the membrane shape around the intercalated inclusions and the corresponding free energy, analytically. We show that the lipid tilt degree of freedom can lead to local softening of the inclusion-containing lipid bilayer segment. The predicted softening requires a sufficiently small value of the tilt modulus; its origin lies in the reduction of the excess membrane-inclusion interaction energy. We compare our results to the case of suppressed microscopic shape relaxation. Here, too, local softening of the membrane is possible.

DOI: 10.1103/PhysRevE.74.051503 PACS number(s): 83.80.Qr, 87.15.Kg

I. INTRODUCTION

Transmembrane proteins can be divided roughly into two groups, flexible (often chainlike) proteins, which cross the membrane bilayer a few times while forming with the interacting lipids flexible complexes, and more rigid globular proteins. In this work, only the second class of proteins, i.e., globular transmembrane proteins, will be considered. For the sake of simplicity, they will be described as rigid objects (or "inclusions") of simple geometrical shapes [1].

A rigid protein, intercalated in a lipid bilayer, perturbs the structure of the surrounding lipids. The corresponding membrane-protein interaction energy is therefore mainly attributed to the change in free energy of the surrounding lipids. As recognized already by Marčelja [2,3], the internal energy of a single lipid depends on the particular sequences of *trans*, *gauche*$^+$, and *gauche*$^-$ conformers along its tail, on the van der Waals interactions of the tail with its neighbors, as well as on steric and electrostatic interactions. Added to that must be a substantial—possibly even dominating [4]—entropic contribution to the free energy that results from the packing properties of lipids in the vicinity of a rigid protein.

The change in the ordering of lipids that surround a protein leads to an indirect, lipid-mediated, interaction between two proteins when they approach each other. A simple and plausible scenario is that on the approach of two proteins, the total lipid perturbation decreases, resulting in a net attractive force and, possibly, protein aggregation [3]. On a more detailed level, it is useful to distinguish between membrane inclusions with and without up-down symmetry [5–7]. The former, such as cylinderlike inclusions, induce a short-range, exponentially decaying, perturbation of the host membrane [3,8–10]. This is in contrast to the latter (among them conelike inclusions), where the absence of a characteristic length scale leads to long-range perturbations and long-range interactions between inclusions. For example, two rigid conelike inclusions experience a membrane-mediated $\sim 1/r^4$ repulsion as function of their distance r [11]. There can also be attraction between conelike inclusions, arising among others due to membrane fluctuation effects [12], due to the opposite orientation of membrane inclusions, or due to lateral membrane tension [13]. Attractive interactions are also predicted for an ensemble of inclusions where multibody effects can lead to quasistable clusters [14,15]. In all cases mentioned thus far, the inclusions are *isotropic*, exhibiting cylindrical symmetry about their axis normal to the membrane. More generally, if cylindrical symmetry is absent, the free energy depends on the inclusion's in-plane orientation within the membrane. Though not the subject of the present work, we mention that the lateral organization of *anisotropic* inclusions can be quite complex, ranging from chainlike assembly [16] and saddlelike membrane regions [17] to periodic pattern formation [18].

Conelike inclusions [1] are characterized by a cone angle onto which the membrane shape has to adapt. On a sufficiently coarse-grained (or mesoscopic) level of the membrane, the inclusion's cone shape can be identified with a local discontinuity in the membrane curvature field. On a more microscopic level, another degree of freedom of the membrane becomes significant, namely, the *tilt* of the lipid molecules [19–21]. Helfrich and Prost [22] have shown that a symmetric lipid bilayer may exhibit an intrinsic bending force if the lipid molecules are collectively tilted. However, membrane perturbations that involve lipid tilt are usually short range with a characteristic length extending only over a few lipids. Lipid tilt is thus important for processes where

*Electronic address: miha.fosnaric@fe.uni-lj.si
†Electronic address: sylvio.may@ndsu.edu

the local membrane geometry changes over short distances, such as for fusion intermediates [23], for nonbilayer lipid phases [24–26], or for the periodic "ripple" phase [27–29]. Also for a membrane that contains rigid inclusions, lipid tilt may be a means to optimize the membrane-inclusion interaction [30]. The resistance of the lipids in a membrane leaflet to tilt and to bend can be described by a tilt modulus κ_t and a bare bending modulus κ_h [19]. Change in tilt gives rise to another deformation mode, *splay*, with corresponding splay modulus κ_s [20]. (Note that the quantities κ_t, κ_h, and κ_s refer to a single monolayer.)

A rigorously flat membrane (characterized, for example, by vanishing spontaneous curvature and $\kappa_h \to \infty$) can still accommodate a conelike inclusion through a tilt deformation. On the other hand, for $\kappa_t \to \infty$, the membrane must accommodate a conelike inclusion through a pure bending deformation with corresponding bending rigidity $\kappa_c = \kappa_h + \kappa_s$. (Here, κ_c is the bending stiffness of a single monolayer as it appears in the familiar Helfrich expression [19] for the curvature free energy.) The intermediate case results in a compromise where the lipid tilt deformation facilitates the matching of the curved membrane to the shape of the inclusion. Characterization of this compromise is one objective of the present work.

A related issue that has received some attention recently is how membrane inclusions affect the curvature elastic properties of the host membrane. Coupling between nonhomogeneous lateral distribution of membrane components and specific membrane shapes may be a general mechanism to generate and stabilize highly curved membrane structures such as spherical buds, membrane necks, and thin tubular membrane protrusions [17,31–35]. On a phenomenological level, membrane bending may couple energetically to the local density of inclusions by introducing a composition-dependent local bending constant and spontaneous curvature. The underlying model (including direct interactions between inclusions and their configurational entropy) was suggested by Markin [31] and used in subsequent applications [36]. Leibler [37] proposed a similar thermodynamic model.

Another theoretical approach [17,38,39] starts from a phenomenological expression for the energy of a *single anisotropic* inclusion (derived by an expansion in terms of the so-called mismatch tensor [40]), which, at the mesoscopic scale, is a function of the two principal membrane curvatures, c_1 and c_2 [17,38,41],

$$E_i = \mu_m + (2K + \bar{K})(H - H_m)^2 - \bar{K}[D^2 - 2DD_m \cos(2\omega) + D_m^2], \quad (1)$$

where μ_m, K, and $\bar{K}$ are phenomenological parameters, $H = (c_1 + c_2)/2$ is the mean curvature, $D = |c_1 - c_2|/2$ is the curvature deviator, whereas $H_m = (c_{1m} + c_{2m})/2$ and $D_m = |c_{1m} - c_{2m}|/2$ are, respectively, the intrinsic mean and deviatoric curvatures that reflect the preferred membrane curvature of the inclusion, measured at the mesoscopic scale. The maximum and minimum of E_i are adopted for an in-plane orientation angle of the inclusion corresponding to $\omega = 0$ and $\omega = \pi/2$, respectively. For $D_m = 0$, Eq. (1) describes the case of

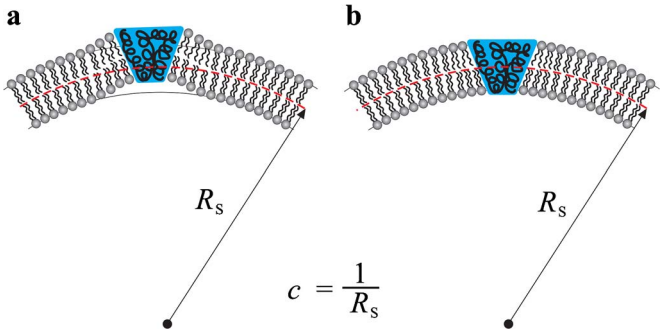

FIG. 1. (Color online) Schematic illustration of a lipid bilayer of prescribed mesoscopic-scale spherical curvature ($c = c_1 = c_2 = H = 1/R_s$) with a conelike intercalated inclusion. In case A, the inclusion induces a local microscopic (nanoscale) membrane shape relaxation, whereas in case B the shape of the membrane does not differ locally from the mesoscopic spherical curvature c of the membrane. In case A, the lipids accommodate the inclusion through the bending deformation and via changes in lipid tilt, whereas in case B the microscopic-level relaxation of the membrane shape is completely suppressed and the inclusion is accommodated only through lipid tilt (see also [41]).

isotropic inclusions. The single-inclusion energy E_i comprises the self-energy of the intercalated inclusion as well as the contribution due to the deformation of the surrounding lipids [17,38,41,42]. We emphasize the mesoscopic level that underlies Eq. (1). That is, the possible microscopic ("nanoscale") perturbation of the membrane shape around the intercalated inclusion, illustrated in Fig. 1(a), is not explicitly taken into account but rather hidden in the phenomenological constants μ_m, K, $\bar{K}$, H_m, and D_m. Applications of the inclusion energy from Eq. (1) include the self-consistent description of equilibrium shapes of a closed bilayer vesicle and the corresponding lateral distribution of intercalated inclusions [17,38,43]. The resulting lateral distribution of inclusions is usually nonhomogeneous, indicating that the equilibrium free energy of the membrane can be lowered through accumulation of inclusions at regions of favorable curvatures [37,38,43]. In accordance with previous results [31], clustering and lateral phase separation of inclusions is additionally enhanced in the presence of direct, attractive, inclusion-inclusion interactions [39]. Moreover, for anisotropic inclusions, the possibility of their orientational ordering within the membrane plane offers an internal degree of freedom that acts toward a decrease of the local bending constant [17,42]. Finally, the influence of inclusions on the (local) curvature elastic properties of a lipid bilayer has been calculated in terms of the properties of the host membrane and the geometry of the intercalated inclusions. It was found [41] that the change in membrane elasticity depends *linearly* on the density of inclusions and that rigid inclusions may either soften of stiffen the host membrane, depending on how strong the interaction with the surrounding lipid bilayer is. The question arises how the elastic behavior of a membrane is affected by the inclusions if the local microscopic membrane shape perturbation (at the nanoscale level) due to each individual inclusion is taken into account [Fig. 1(a)]. Answering this question is another objective of the present work.

In general, the theoretical description of local microscopic perturbations of lipid molecules around an intercalated inclusion falls in between two limiting cases. In the first case the inclusions are distributed over the whole surface of a *closed* membrane (or at least over a major part of it). Here, a local, microscopic, perturbation of the membrane shape around each of the rigid inclusions [as schematically shown in Fig. 1(a)] would greatly increase the nonlocal bending energy of the bilayer membrane (also called the relative stretching energy since it originates from different degree of stretching of both monolayers during bending of the bilayer at constant average membrane area) [44–46]

$$W_n = k_n A(\langle H\rangle - H_0)^2, \tag{2}$$

where $\langle H\rangle = \int H dA/A$ is the average mean curvature, H_0 is the spontaneous mean curvature [34], k_n is the coefficient of nonlocal bending rigidity [46], A is the membrane area, and dA is the membrane area element. For a closed, nearly flat, bilayer membrane (where $\langle H\rangle \approx 0$, $H_0 \approx 0$), with N homogeneously distributed intercalated inclusions, the membrane's nonlocal bending energy W_n can be approximately written as

$$W_n \cong k_n A(N\langle H\rangle_p - NH_{0p})^2 \propto N^2, \tag{3}$$

where H_{0p} and $\langle H\rangle_p$ refer to the disturbed membrane patch around the single membrane-intercalated inclusion [Fig. 1(a)]. Note that the energy W_n increases quadratically with the number of membrane-embedded inclusions. For large enough N, the local microscopic perturbation of the membrane shape around each intercalated inclusion [schematically shown in Fig. 1(a)] becomes energetically unfavorable. Thus, the membrane shape remains locally unperturbed [Fig. 1(b)], and the lipids accommodate the inclusion only through lipid tilt.

The opposite limit corresponds to an open system, where the inclusions are spatially confined to a small membrane segment, always maintaining contact with a large reservoir of a relaxed bare lipid bilayer. Here, the lipids surrounding the inclusion are free to adjust their conformation also by optimizing the local membrane shape near the inclusion, as schematically shown in Fig. 1(a). Analysis of this latter case is the main subject of the present work.

To render the problem tractable, we shall adopt one major (but not uncommon [9,10]) approximation: a cell model, i.e., we shall assume that the inclusions are homogeneously distributed over a membrane segment of *prescribed* spherical curvature ($c_1 = c_2 = c$), defined at the mesoscopic level. The cell model starts from a hexagonal arrangement of spatially fixed conelike inclusions of (average) radius r_0 (see Fig. 4). It approximates the corresponding (hexagonally symmetric) Wigner-Seitz cell by a (cylindrically symmetric) circle of radius approximately half the separation between neighboring inclusions (see Fig. 3). The radius R of the unit cell then defines the (uniform) area fraction $m = r_0^2/R^2$ of inclusions in the membrane segment. Our aim is to characterize—at the mesoscopic scale—the bending stiffness of an inclusion-containing membrane patch with prescribed spherelike membrane curvature. Hence, the membrane curvatures at the boundaries of each unit cell are fixed to be $c_1 = c_2 = c$, where c corresponds to the spherelike (mesoscopic-level) membrane curvature c; see Fig. 1. The fact that the curvatures at the cell boundaries are all equal is a consequence of both the symmetry of the deformation and the isotropy of the inclusions. Yet, the local, microscopic, membrane shape perturbation within the unit cell is allowed to minimize the membrane free energy (see also Fig. 3).

The bending stiffness of the inclusion-containing membrane will be characterized by a modulus κ that appears in a quadratic curvature expansion $\hat{f} = \kappa c^2/2$ of the free energy density, measured per unit area. In terms of the commonly used Helfrich expression [19] for the bending free energy density of a bilayer membrane $\hat{f} = 2\kappa_c(c_1 + c_2 - c_0)^2/2 + 2\bar{\kappa} c_1 c_2$ [where $2\kappa_c$, $2\bar{\kappa}$, and c_0 are the (local) bending modulus, the Gaussian modulus, and the spontaneous curvature, respectively]—the individual quantities κ_c and $\bar{\kappa}$ refer to a single monolayer—the relevant modulus here is (because of $c_1 = c_2 = c$) given by $\kappa = 8\kappa_c + 4\bar{\kappa}$. One of the major results of the present work will be an analytical expression for κ as a function of the inclusion density m. In fact, it will turn out to be more convenient to express κ as a function of the relative cell size $\rho = R^2/r_0^2 - 1$, implying $\rho = (1-m)/m$ or, equivalently, $m = 1/(1+\rho)$. We will show that inclusions can locally either increase or decrease κ depending on m and on the material properties of the host membrane. The tilt modulus κ_t plays a crucial role in determining whether inclusions render the membrane more rigid or more flexible. For example, the commonly considered limit $\kappa_t \to \infty$ always leads to membrane stiffening, whereas the opposite limit $\kappa_t \to 0$ can still lead to either softening or stiffening. We also analyze the role of the Gaussian modulus $\bar{\kappa}$ and the situation where the local microscopic membrane shape perturbations are restricted [the latter corresponding to Fig. 1(b)]. Finally, the phenomenological parameters K, $\bar{K}$, and H_m, describing the single inclusion energy in the mesoscopic curvature field of the membrane [Eq. (1)], are estimated.

II. THEORETICAL MODEL AND RESULTS

A. Elastic energy of a perturbed membrane

We consider a lipid membrane that consists of two apposed monolayers, an external (E) and an internal (I) one. Both monolayers are described by a height profile, h_E and h_I, and by their local directors (unit vectors), $\mathbf{t}_E$ and $\mathbf{t}_I$, that describe the average orientation of the lipid chains; see Fig. 2. We assume a weakly perturbed membrane with respect to the flat state where both h_E and h_I are constant (e.g., parallel to the x,y plane of a Cartesian coordinate system) and where all directors point normal to the monolayer interfaces (parallel to the z axis).

The elastic free energy per unit area, $\hat{f}_E$, of the external monolayer can be written up to quadratic order in h_E and $\mathbf{t}_E$ as

$$\hat{f}_E = \frac{\kappa_s}{2}(\nabla \cdot \mathbf{t}_E)^2 + \frac{\kappa_t}{2}(\mathbf{t}_E - \nabla h_E)^2 + \frac{B}{2}(h_E - h)^2 + \frac{\kappa_h}{2}(\Delta h_E)^2 + \frac{K}{2}(\nabla \times \mathbf{t}_E)^2 + \bar{\kappa} \det h_{E,ij}. \tag{4}$$

The first term in Eq. (4) characterizes the splay energy of the lipid chains with κ_s being the corresponding splay modulus. The second term accounts for the energy cost of tilting the director $\mathbf{t}_E$ away from its orientation normal to the surface h_E; the prefactor κ_t is the tilt modulus. Thickness changes of the monolayer are accounted for by the third term, where B is the compression modulus and h is a reference surface with respect to which the compression/expansion of the monolayer is measured. It is reasonable to assume that for given membrane thickness h_E-h_I the thickness of each monolayer is allowed to relax; this specifies $h=(h_E+h_I)/2$ to be the average height profile of the bilayer. The fourth term in Eq. (4) expresses the bare bending energy of the external monolayer with corresponding modulus κ_h. Note that this term is distinct from the splay energy; only for $\kappa_t \to \infty$ splay and bare bending refer to the same deformation. The splay energy mainly accounts for the splay deformation of the lipid chains, whereas the bending term originates predominantly in the head-group region of the monolayer. For example, the electrostatic contribution to the bending modulus contributes entirely to κ_h. One might therefore refer to the modulus κ_h as the head-group contribution to the bending stiffness. The last two terms in Eq. (4) describe the energetic contribution of a twist deformation of the chains (with corresponding modulus K) and of a saddle deformation of h_E (with modulus $\bar{\kappa}$). We note that Eq. (4) agrees with the free energy expansion derived by Fournier [21]. The only difference is that the three individual terms involving $\mathbf{t}_E^2$, $\mathbf{t}_E \nabla h_E$, and $(\nabla h_E)^2$ are combined in Eq. (4) as $(\mathbf{t}_E-\nabla h_E)^2$, which accounts for tilt resistance only with respect to the normal direction of the corresponding external membrane leaflet. This is justified by the fluidlike hydrocarbon core of the lipid bilayer and thus the weak energetic intermonolayer coupling of the lipid directors.

Starting from $\hat{f}_E$, we obtain the elastic free energy of the internal leaflet, $\hat{f}_I$, by replacing $h_E \to h_I$ and $\mathbf{t}_E \to -\mathbf{t}_I$ (the minus sign in the latter reflecting the opposite orientation of the two apposed monolayers). Hence,

$$\hat{f}_I = \frac{\kappa_s}{2}(\nabla \cdot \mathbf{t}_I)^2 + \frac{\kappa_t}{2}(\mathbf{t}_I + \nabla h_I)^2 + \frac{B}{2}(h_I - h)^2 + \frac{\kappa_h}{2}(\Delta h_I)^2 + \frac{K}{2}(\nabla \times \mathbf{t}_I)^2 + \bar{\kappa} \det h_{I,ij}. \quad (5)$$

The elastic free energy of the lipid bilayer per unit area is then $\hat{f}_{bl}=\hat{f}_E+\hat{f}_I$.

At this point it is convenient to switch to a new set of variables, namely, to the average shape h and thickness dilation u, defined through $h_E=h+u$ and $h_I=h-u$. Similarly, we define the average director $\mathbf{t}$ and the difference director $\mathbf{d}$ via the relations $\mathbf{t}_E=\mathbf{t}+\mathbf{d}$ and $\mathbf{t}_I=\mathbf{t}-\mathbf{d}$. This allows us to express $\hat{f}_{bl}=\hat{f}_{tu}+\hat{f}_{dh}$ as the sum of the two independent contributions [21]

$$\hat{f}_{tu} = \kappa_s(\nabla \cdot \mathbf{t})^2 + \kappa_t(\mathbf{t} - \nabla u)^2 + Bu^2 + \kappa_h(\Delta u)^2 + K(\nabla \times \mathbf{t})^2 + 2\bar{\kappa} \det u_{,ij} \quad (6)$$

and

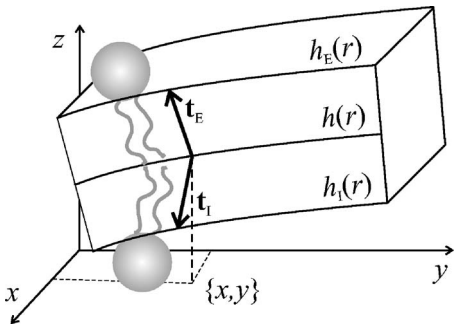

FIG. 2. Illustration of a perturbed lipid bilayer with indicated local directors $\mathbf{t}_E$ and $\mathbf{t}_I$ and height profiles h_E and h_I of the external and internal leaflet, respectively. The average height of the bilayer is $h=(h_E+h_I)/2$. Two lipid molecules are shown schematically.

$$\hat{f}_{dh} = \kappa_s(\nabla \cdot \mathbf{d})^2 + \kappa_t(\mathbf{d} - \nabla h)^2 + \kappa_h(\Delta h)^2 + K(\nabla \times \mathbf{d})^2 + 2\bar{\kappa} \det h_{,ij}. \quad (7)$$

The two contributions can be treated separately. The first one depends on the tilt difference $\mathbf{t}$ and thickness dilation u, which is relevant for inclusions with up-down symmetry, including the case of hydrophobic mismatch. The corresponding inclusion-induced deformation is short range and has been studied intensively in the past (see Introduction). In the present work, we focus our interest entirely on the second contribution [namely, Eq. (7)]. In other words, we consider membrane deformations due to isotropic, conelike inclusions with no hydrophobic mismatch (implying $\hat{f}_{tu}=0$). We thus seek to minimize the overall elastic free energy $F_{dh}=\int \hat{f}_{dh} da$, where $da=dxdy[1+(\nabla h)^2]^{1/2}$ denotes the area element of the lipid bilayer. The corresponding Euler-Lagrange equations pertaining to F_{dh} are

$$\kappa_t(\mathbf{d} - \nabla h) - \kappa_s \nabla(\nabla \cdot \mathbf{d}) + K \nabla \times (\nabla \times \mathbf{d}) = 0,$$

$$\kappa_h \nabla^4 h + \kappa_t(\nabla \cdot \mathbf{d} - \Delta h) = 0. \quad (8)$$

In the following, we solve these equations for cylindrical symmetry and calculate the corresponding free energy F_{dh}.

B. Array of conelike inclusions

The assumption of cylindrical symmetry for the deformation of the membrane around each inclusion is a frequently used approximation to account for the multibody nature of membrane-mediated inclusion-inclusion interactions. As mentioned in the Introduction, it corresponds to approximating the Wigner-Seitz cell of a hexagonal inclusion arrangement by a circle; see Fig. 3. For the radius of the circle we adopt the convenient choice $R=0.5\lambda$ (a more accurate value would be $R=0.525\lambda$), where λ is the distance between two neighboring inclusions in a hexagonal array. Another assumption is that the array of inclusions is in contact with a reservoir of lipid molecules, so that there is no further constraint on the number of lipid molecules. Hence, no influences of nonlocal bending elasticity [Eq. (2)] and area stretching of the lipid bilayer [19,45] are accounted for in the present work. Our assumptions render the following analysis

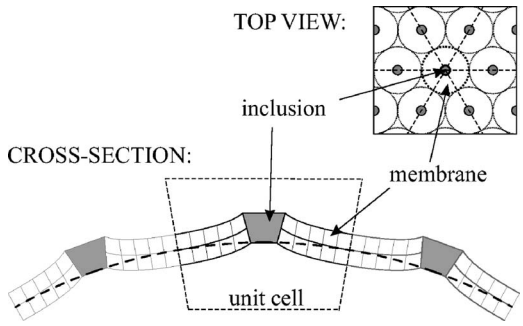

FIG. 3. Top view: A hexagonal array of laterally fixed isotropic conelike inclusions (shaded circles); the unit cell around each inclusion is approximated by a circle. The depiction of the membrane shape in the cross section is based on an actual calculation with cone angle $d_0=-15°$, cell radius $R=10$ nm, and an angle $cR=10°$ that defines the imposed spherical mesoscopic membrane curvature c (broken line). All other parameters are as in Fig. 5(c). The shaded cones represent cross sections through the inclusions.

somewhat less general but allow us to calculate an analytical expression for F_{dh}.

The cylindrical symmetry of the unit cell suggests to use cylindrical coordinates $\{r,\phi\}$. Then, only the radial components, $d(r)$ of $\mathbf{d}$ and $\nabla_r h(r)$ of ∇h, are nonvanishing. Figure 4 shows a cross section through the unit cell with the two order parameters, the height profile $h(r)$ and the difference director $d(r)$, indicated. Up to second order in the two-order parameters $d(r)$ and $h(r)$ (and their derivatives), the free energy per unit cell $F_{dh}=\int \hat{f}_{dh} da$ [with $\hat{f}_{dh}$ specified in Eq. (7)] reads

$$\frac{F_{dh}}{2\pi\kappa_s} = \int_{r_0}^{R} dr r \left[\frac{\omega^2\eta^2}{1+\eta^2}(d-\nabla_r h)^2 + (\nabla_r \cdot d)^2 + \eta^2(\nabla_r^2 h)^2 \right] + 4\bar{\alpha}(1+\eta^2)\int_{r_0}^{R} h' h'' dr, \tag{9}$$

where the radius of the inclusion is r_0, the cell radius is R, and where we have defined $\eta^2=\kappa_h/\kappa_s$, $\bar{\alpha}=\bar{\kappa}/[2(\kappa_s+\kappa_h)]$, and

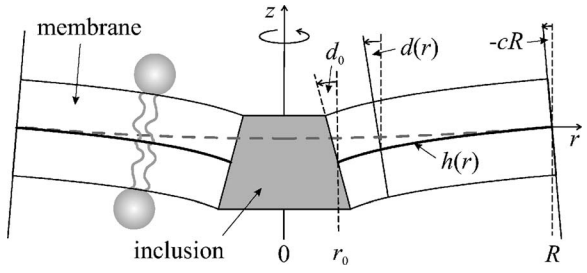

FIG. 4. A cylindrically symmetric unit cell containing a single cone-shaped inclusion. The calculated shape $h(r)$ of the locally perturbed membrane with prescribed (mesoscopic-level) curvature c is shown as the two thick solid lines. Here, the cone angle of the inclusion is $d_0=15°$, the angle defining the prescribed curvature is $cR=-5°$, and the radius of the unit cell is $R=5$ nm. All other parameters are the same as in Fig. 5(c). The dashed line shows $h(r)$ for an inclusion-free membrane with curvature c.

$\omega^2=\kappa_t/\kappa_s+\kappa_t/\kappa_h$. It follows that $\omega^2\eta^2/(1+\eta^2)=\kappa_t/\kappa_s$. Note that the prime denotes the derivative with respect to r and ∇_r denotes the radial component of the nabla operator. Thus, $\nabla_r h=h'(r)$, $\nabla_r^2 h=[rh'(r)]'/r$, and $\nabla_r\cdot d=[rd(r)]'/r$. The Euler-Lagrange equations [see Eqs. (8)] now read

$$\frac{\omega^2\eta^2}{1+\eta^2}(d-\nabla_r h)-\nabla_r(\nabla_r\cdot d)=0$$

$$\nabla_r^4 h+\frac{\omega^2}{1+\eta^2}(\nabla_r\cdot d-\nabla_r^2 h)=0. \tag{10}$$

The boundary conditions at $r=R$ are

$$h(R)=0, \quad \nabla_r h(R)=-cR, \quad d(R)=-cR. \tag{11}$$

The first boundary condition specifies the reference point for measuring the height profile, the second imposes the mesoscopic curvature c of the membrane (see also Fig. 1), and the third, which corresponds to vanishing tilt at $r=R$, ensures smoothness of the membrane at the cell boundary. At the inclusion rim, the boundary conditions are

$$d(r_0)=d_0, \quad \nabla_r^2 h(r_0)+2\bar{\alpha}\frac{1+\eta^2}{\eta^2}\frac{h'(r_0)}{r_0}=0.$$

$$d(r_0)-\nabla_r h(r_0)+\frac{1+\eta^2}{\omega^2}\nabla_r^3 h(r_0)=0. \tag{12}$$

The first expresses the matching of the difference director at $r=r_0$ to the cone angle d_0 of the inclusion; see Fig. 4. The second and third expressions are the natural boundary conditions that allow optimization of $h(r_0)$ and $\nabla_r h(r_0)$.

Using the Euler-Lagrange equations and the boundary conditions, Eqs. (11) and (12), we can carry out the integrations in Eq. (9), resulting in

$$\frac{F_{dh}}{2\pi\kappa_s}=-cR^2\nabla_r d(R)-r_0 d_0\nabla_r d(r_0)-cR^2\eta^2\nabla_r^2 h(R) + 2\bar{\alpha}(1+\eta^2)[\nabla_r h(R)]^2. \tag{13}$$

On the other hand, we can write F_{dh} as an expansion with respect to the prescribed spherelike reference curvature $c=c_1=c_2$ as

$$F_{dh}=F_{\mathrm{opt}}+\pi R^2\frac{\kappa}{2}(c-c_0)^2, \tag{14}$$

which contains three constants: the optimal (spherelike) curvature c_0 (defined at a mesoscopic level), the bending stiffness for spherical deformations κ, and the elastic free energy for optimal curvature $F_{\mathrm{opt}}=F_{dh}(c=c_0)$.

Consider first an inclusion-free membrane. Here, $r_0=0$, and the boundary conditions in Eq. (12), must be replaced by $d(0)=0$, $\nabla_r h(0)=0$, and $\nabla_r^3 h(0)=0$, which follow from the smoothness and compactness of the inclusion-free membrane at $r_0=0$. We find that there is no tilt of the lipid directors and a uniform curvature of the membrane. The former implies $d(r)=\nabla_r h(r)$ and the latter $h(r)=c(R^2-r^2)/2$. The two main

curvatures, $c_1=-h'(r)/r=c$ and $c_2=-h''(r)=c$, are thus equal to each other. The elastic free energy $F_0=F_{dh}$ in the absence of an inclusion is

$$\frac{F_0}{2\pi\kappa_s}=2(1+\eta^2)(1+\bar{\alpha})R^2c^2. \tag{15}$$

We thus find $F_{\mathrm{opt}}=0$, $c_0=0$, and $\kappa=\kappa_0=8\kappa_s(1+\eta^2)(1+\bar{\alpha})=8(\kappa_s+\kappa_h)+4\bar{\kappa}$. The latter relation, $\kappa_0=8\kappa_c+4\bar{\kappa}$, was already stated in the Introduction. We introduce the inclusion-induced relative change of the membrane's bending stiffness for spherical deformation

$$\kappa_{\mathrm{rel}}=\frac{\kappa}{\kappa_0}-1. \tag{16}$$

For $\kappa_{\mathrm{rel}}>0$ ($\kappa_{\mathrm{rel}}<0$), the inclusion stiffens (softens) the membrane. The hypothetical case of vanishing stiffness ($\kappa=0$) corresponds to $\kappa_{\mathrm{rel}}=-1$.

Also, for an inclusion-containing membrane, we can derive analytical expressions for the bending constant, the optimal (spherelike) curvature, and the elastic energy for optimal curvature. To this end we solve the Euler-Lagrange equations, Eqs. (10), subject to the boundary conditions, Eqs. (11) and (12), and insert the solutions for $h(r)$ and $d(r)$ into F_{dh} in Eq. (13). The final results for F_{opt}, c_0, and κ_{rel} can be written in terms of the relative cell size $\rho=(R/r_0)^2-1$ and the quantities $\tilde{\eta}=(1+\eta^2)/\eta^2=(\kappa_s/\kappa_h)+1$ and

$$P=\frac{2}{\omega r_0}\frac{I_1(\omega R)K_1(\omega r_0)-I_1(\omega r_0)K_1(\omega R)}{I_1(\omega R)K_0(\omega r_0)+I_0(\omega r_0)K_1(\omega R)}, \tag{17}$$

where I_n and K_n give the modified Bessel functions of the first and second kind, respectively. We find

$$\frac{F_{\mathrm{opt}}}{2\pi\kappa_s}=\frac{-2\bar{\alpha}d_0^2\{(1+\eta^2)(1+\bar{\alpha})\rho+P\bar{\alpha}\tilde{\eta}\}}{1+\rho(1+\bar{\alpha})+P\bar{\alpha}\eta^2\{1-\tilde{\eta}^2[1+\rho(1+\bar{\alpha})]\}}, \tag{18}$$

$$\frac{R^2c_0}{d_0r_0}=\frac{-(1-P\bar{\alpha}\tilde{\eta})(1+\rho)}{1+\rho(1+\bar{\alpha})+P\bar{\alpha}\eta^2\{1-\tilde{\eta}^2[1+\rho(1+\bar{\alpha})]\}}, \tag{19}$$

and

$$\kappa_{\mathrm{rel}}=\frac{1}{1+\bar{\alpha}}\frac{1-P\eta^2(1+\bar{\alpha}\tilde{\eta}^2)}{\rho+P\eta^2(1-\bar{\alpha}\tilde{\eta}^2\rho)}. \tag{20}$$

These expressions, particularly that for κ_{rel}, are the main result of this work. In the following, we analyze the influence of r_0, R, η, ω, and $\bar{\alpha}$ on κ_{rel}, focusing on the question whether rigid isotropic inclusions (which are homogeneously distributed over a small membrane patch with prescribed mesoscopic spherical curvature) act toward rigidification ($\kappa_{\mathrm{rel}}>0$) or softening ($\kappa_{\mathrm{rel}}<0$) of this membrane patch.

We note that κ_{rel} is independent of d_0. Hence, within our cell model, the effect of rigid, isotropic inclusions on the local membrane elasticity does depend on the inclusion size but not on the inclusion shape. In other words, cylinderlike and conelike inclusions influence the bending stiffness κ in the same manner.

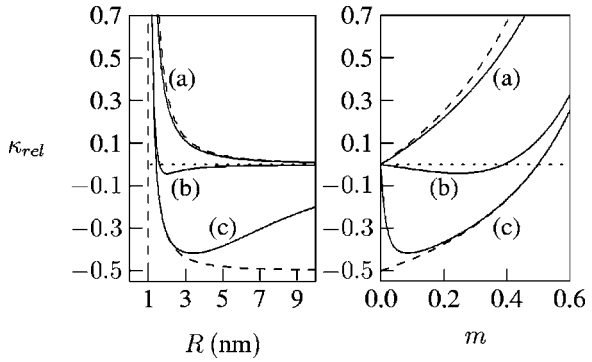

FIG. 5. The inclusion-induced relative change in membrane stiffness, κ_{rel}, according to Eq. (22), plotted as a function of R (left graph) and $m=r_0^2/R^2$ (right graph) for (a) $\omega=20/\mathrm{nm}$, (b) $\omega=2/\mathrm{nm}$, and (c) $\omega=0.2/\mathrm{nm}$. The remaining parameters are $\eta=1$, $r_0=1$ nm, and $\bar{\alpha}=0$. The upper and lower broken lines correspond to Eqs. (23) and (24), respectively. The limiting value for $R\to\infty$ (or equivalently $m=0$) of the lower broken line is according to Eq. (24) (with $\rho\to\infty$) given by $\kappa_{\mathrm{rel}}=-\eta^2/(1+\eta^2)=-1/2$.

C. Vanishing Gaussian modulus

We first discuss the case of vanishing Gaussian modulus, $\bar{\kappa}=0$, implying $\bar{\alpha}=0$. In this case, the result for F_{dh} simplifies considerably and is given by

$$\frac{F_{dh}}{2\pi\kappa_s}=\frac{2(1+\eta^2)}{\rho+\eta^2P}(d_0+cR^2/r_0)^2 \tag{21}$$

from which we conclude $F_{\mathrm{opt}}=0$, $c_0=-d_0r_0/R^2=-md_0/r_0$, and

$$\kappa_{\mathrm{rel}}=\frac{1-\eta^2P}{\rho+\eta^2P}. \tag{22}$$

The case $F_{dh}=0$ for the optimal curvature $c=c_0=-d_0r_0/R^2$ is particularly simple. Here, we find $h(r)=d_0r_0\ln(r/R)$ and $d(r)=\nabla_r h(r)=d_0r_0/r$, implying no tilt deformation of the lipid tails and a catenoidlike saddle geometry for the membrane that matches both the inclusion shape at r_0 and the imposed geometry at R.

To motivate the following discussion we plot κ_{rel} for some cases that represent a typical lipid membrane. In the absence of experimental data, estimations of the splay and bare contribution to the bending stiffness yield for κ_s and κ_h the same order of magnitude of a few kT [21], where kT denotes the thermal energy unit. Here we assume $\kappa_s=\kappa_h=5$ kT, implying $\eta=1$. For the inclusion radius, we set $r_0=1$ nm. A reasonable choice for the tilt modulus is $\kappa_t=10\ \mathrm{kT/nm^2}$ [47], implying $\omega=2/\mathrm{nm}$. Curve (b) in Fig. 5 shows κ_{rel} as a function of the cell size R (left diagram) and area fraction $m=r_0^2/R^2$ of the inclusions (right diagram). In addition, Figure 5 also shows κ_{rel} for $\omega=20/\mathrm{nm}$ [curve (a)] and $\omega=0.2/\mathrm{nm}$ [curve (c) in Fig. 5], corresponding to very small ($\kappa_t=0.1\ \mathrm{kT/nm^2}$) and very large ($\kappa_t=1000\ \mathrm{kT/nm^2}$) tilt modulus, respectively. Fig-

ure 5 suggests that, depending on the tilt modulus, inclusions are principally able to locally either stiffen or soften the host membrane segment. Particularly the possibility of local membrane *softening* is a notable and, at the first glance, an unexpected result. It adds another, previously unrecognized, mechanism of inclusion-induced membrane softening. The softening applies to a membrane bilayer segment with homogeneously distributed rigid inclusions and is a consequence of the finite inclusion size. That is, on insertion of inclusions, a lateral flow of lipid molecules must take place out of the membrane patch into the surrounding, stress relaxed, bilayer membrane where these lipids do no longer participate in the bending deformation.

Let us now analyze the analytical expression for κ_{rel} as given in Eq. (22). The key role for the local softening of a membrane segment with homogeneously distributed inclusions is played by the tilt modulus κ_t (or equivalently by ω). We note the two limits

$$\kappa_{\mathrm{rel}}(\omega \to \infty) = \frac{1}{\rho} \tag{23}$$

and

$$\kappa_{\mathrm{rel}}(\omega = 0) = \frac{1}{\rho}\left[1 - \frac{\eta^2}{1+\eta^2}(1+\rho)\right]. \tag{24}$$

[These are the two extreme cases displayed graphically for $r_0=1$ nm in Fig. 5 by the two broken lines, the upper one referring to Eq. (23) and the lower one to Eq. (24) with $\eta=1$.] Also notable are the two limits for the bare bending stiffness κ_h (or equivalently η). They follow immediately from Eq. (22) and are given by $\kappa_{\mathrm{rel}}(\eta=0)=1/\rho$, signifying membrane stiffening, and $\kappa_{\mathrm{rel}}(\eta\to\infty)=-1$. The latter result does not commute with Eq. (23). It requires a finite tilt modulus so that a rigid inclusion can be incorporated into an infinitely stiff membrane through a tilt deformation. Similarly, Eq. (23) demands a finite η so that a bare membrane bending deformation is still possible.

From Eqs. (23) and (24), we draw two conclusions. First, ignoring the lipid tilt degree of freedom (which corresponds to $\kappa_t\to\infty$ and thus $\omega\to\infty$) always implies inclusion-induced local stiffening of the membrane according to $\kappa_{\mathrm{rel}}=1/\rho=m/(1-m)$. Hence, for small area fraction m of inclusions in the membrane $\kappa_{\mathrm{rel}}=m$, independent of any other material properties. Second, for negligible resistance against a tilt deformation ($\omega=0$), Eq. (24) predicts local softening (that is $\kappa_{\mathrm{rel}}<0$) for sufficiently large cell size, namely, for $R > r_0\sqrt{(1+\eta^2)/\eta^2}$. (Hence, the lower broken lines in both diagrams of Fig. 5 intersect with $\kappa_{\mathrm{rel}}=0$ at $R=\sqrt{2}$ nm corresponding to $m=1/2$.)

Consider now the case of intermediate ω. For which region of R do we find softening and when is the membrane rigidified? We find a simple answer in the limit of large inclusions where $\omega r_0 \gg 1$. Because $R > r_0$, we then also have $\omega R \gg 1$. Using the asymptotic behaviors of the modified Bessel functions

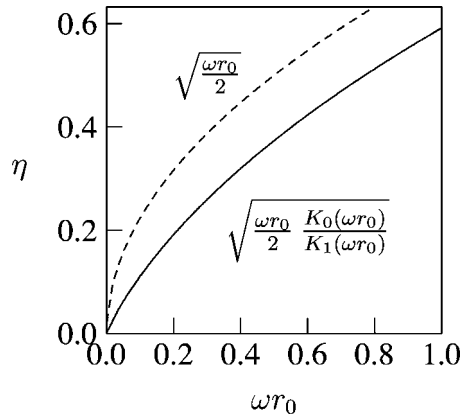

FIG. 6. The functions $\eta(\omega r_0)=\sqrt{(\omega r_0/2)K_0(\omega r_0)/K_1(\omega r_0)}$ [solid line; see Eq. (28)] and $\eta(\omega r_0)=\sqrt{\omega r_0/2}$.

$$I_n(x \gg 1) = e^x \frac{1}{\sqrt{2\pi x}}, \quad K_n(x \gg 1) = e^{-x}\sqrt{\frac{\pi}{2x}}, \tag{25}$$

we find

$$\kappa_{\mathrm{rel}} = \frac{R^2}{R^2 - r_0^2 + \dfrac{2\eta^2 r_0}{\omega}\tanh[\omega(R-r_0)]} - 1. \tag{26}$$

In this case, $\kappa_{\mathrm{rel}}=0$ implies

$$\frac{2\eta^2}{\omega r_0} = \coth[\omega(R-r_0)]. \tag{27}$$

Hence, the smallest value for η^2 that fulfills $\kappa_{\mathrm{rel}}=0$ is $\eta^2=\eta_c^2=\omega r_0/2$, adopted for $R \gg r_0$. We note that because of our assumption $\omega r_0 \gg 1$, it is also $\eta_c^2 \gg 1$. In other words large inclusions would only be able to locally soften the membrane segment if $\kappa_h \gg \kappa_s$. However, such a relation is not expected to be fulfilled for a lipid membrane.

Abandoning the condition of large inclusions, we find from Eq. (22) for $\kappa_{\mathrm{rel}}=0$ the condition $\eta^2 P=1$. Here again, the smallest value for η^2 that fulfills $\kappa_{\mathrm{rel}}=0$ is adopted for $R \gg r_0$. It is given by the relation

$$\frac{2\eta^2}{\omega r_0} = \frac{K_0(\omega r_0)}{K_1(\omega r_0)}, \tag{28}$$

which is displayed in Fig. 6 (solid line) together with the large inclusion approximation $K_0(\omega r_0)=K_1(\omega r_0)$ (broken line). We conclude that for small inclusions (where $\omega r_0 \ll 1$) small values of η are sufficient to induce local softening of membrane segments by inclusions. [We note the limiting behavior $\eta^2=-(\omega^2 r_0^2/2)\ln(\omega r_0/2)$ for $\omega r_0 \ll 1$]. Curve (b) in Fig. 5 confirms that for a supposedly reasonable choice of the elastic moduli of a lipid membrane one can easily obtain (a small but notable) inclusion-induced softening of the membrane segment. For small tilt modulus, the softening can be substantial.

D. Influence of the Gaussian modulus

Up to this point, we were concerned with vanishingly small Gaussian modulus ($\bar{\kappa}=0$), implying $\bar{\alpha}=0$. In the fol-

lowing, we discuss the case $\bar{\kappa}<0$ or, equivalently, $\bar{\alpha}<0$. The range within which $\bar{\alpha}$ can vary should ensure stability of the inclusion-free membrane, implying

$$-1<\bar{\alpha}<0. \tag{29}$$

The first inequality follows from the stability with respect to a spherelike membrane deformation (where $c_1=c_2=c$); see Eq. (15). The second inequality ensures stability with respect to a saddlelike membrane bilayer deformation (where $c_1=-c_2$).

Recall that the Euler-Lagrange equations, Eqs. (10), do not depend on $\bar{\alpha}$, which is a manifestation of the Gauss-Bonnet theorem. However, the free energy F_{dh} in Eq. (9) does depend on $\bar{\alpha}$ because of the natural boundary conditions that optimize $h(r_0)$ and $h'(r_0)$ [see Eqs. (12)]. In the limit of infinite tilt modulus, the inclusion-induced relative change in the bending stiffness for spherical deformation is

$$\kappa_{\mathrm{rel}}(\omega\to\infty)=\frac{1}{1+\bar{\alpha}}\frac{1}{\rho} \tag{30}$$

or, equivalently,

$$\kappa(\omega\to\infty)=\frac{8(\kappa_s+\kappa_h)}{1-r_0^2/R^2}+4\bar{\kappa}. \tag{31}$$

This result generalizes Eq. (23). It shows that in the limit of infinite ω a nonvanishing Gaussian modulus $(-1<\bar{\alpha}<0)$ increases κ_{rel}. This is because the Gaussian part of the bending stiffness for spherical deformations (which reduces κ, since $\bar{\kappa}<0$) is not affected by the presence of an inclusion [see Eq. (31)].

Two other limiting cases, for small and large κ_h, can also be derived from Eq. (20). For $\eta=0$, we obtain $\kappa_{\mathrm{rel}}=1/[\rho(1+\bar{\alpha})]$ and $\eta\to\infty$ implies $\kappa_{\mathrm{rel}}=-1/(1-\bar{\alpha}\rho)$. Both results—the former being identical to the limit $\omega\to\infty$ as specified in Eq. (30)—imply an additional rigidification of the inclusion-containing membrane segment due to a nonvanishing Gaussian modulus $\bar{\kappa}<0$.

A numerical analysis suggests that the increase of κ_{rel} with increasing magnitude of the Gaussian modulus is a general property, also valid for finite values of ω. As an illustration, Fig. 7 shows some numerical results. It appears that the Gaussian modulus acts effectively toward rigidification of the inclusion-containing membrane segment. Note that the value of the Gaussian modulus is not known for most bare lipid membranes (for experimentally deduced values of $\bar{\kappa}$ see [48] and the references in [49]).

E. Membrane segment with uniform local curvatures

The present work analyzes the consequences that the lipid tilt degree of freedom has on a membrane that contains rigid conelike inclusions. As discussed in the Introduction, it is a common approach to ignore this degree of freedom and to base the analysis of the local free energy entirely on the Helfrich bending free energy [which corresponds to the limit $\kappa_t\to\infty$ as analyzed above; see Eqs. (23) and (30)]. Also, a complementary approach has been considered recently where the microscopic optimization of the membrane shape is suppressed. Here, an inclusion can be accommodated into the host membrane by the tilt degree of freedom of the lipids [41,42]. More specifically, an inclusion interacts with a small membrane segment of uniform *local* curvature [Fig. 1(b)]. Our present approach allows us—at least for prescribed spherical curvature of the membrane segment (Fig. 1)—to consider this case and to compare it to that of unconstrained local curvatures.

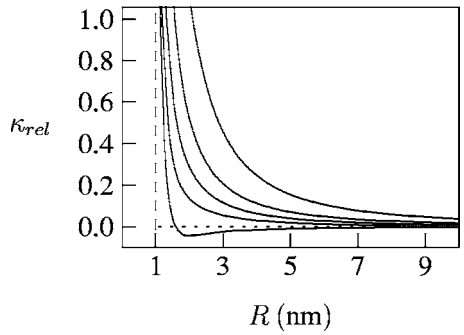

FIG. 7. The inclusion-induced relative change in membrane stiffness, κ_{rel}, for a spherical membrane segment with homogeneously distributed inclusions, plotted as a function of R for $\bar{\alpha}=0$, −0.2, −0.4, −0.6, −0.8 (solid lines from bottom to top). The parameters are $\omega=2/\mathrm{nm}$, $\eta=1$, and $r_0=1$ nm. The curve for $\bar{\alpha}=0$ corresponds to curve (b) in Fig. 5.

We thus consider a membrane segment with homogeneous curvatures, $c=c_1=c_2$. That is we *assume* all local curvatures of an inclusion-containing membrane segment to be uniform [as illustrated in Fig. 1(b)]. Equivalently expressed, we consider the case where the local microscopic shape relaxation of the membrane is suppressed. The expression for the corresponding membrane free energy per unit cell follows from inserting the shape of an inclusion-free membrane $h(r)=c(R^2-r^2)/2$ into Eq. (9), resulting in

$$\frac{F_{dh}}{2\pi\kappa_s}=\int_{r_0}^{R}drr\left[\tilde{\omega}^2(d+cr)^2+\left(d'+\frac{d}{r}\right)^2+4\eta^2c^2\right]+4\bar{\alpha}(1+\eta^2)\int_{r_0}^{R}c^2drr, \tag{32}$$

where we have defined $\tilde{\omega}^2=\omega^2\eta^2/(1+\eta^2)=\kappa_t/\kappa_s$. In equilibrium, the function $d(r)$ must fulfill the Euler-Lagrange equation $\tilde{\omega}^2(d+cr)=[d'+d/r]'$ subject to the boundary conditions $d(r_0)=d_0$ and $d(R)=-cR$. The solution is

$$d(r)=(d_0+cr_0)\frac{I_1(\tilde{\omega}R)K_1(\tilde{\omega}r)-I_1(\tilde{\omega}r)K_1(\tilde{\omega}R)}{I_1(\tilde{\omega}R)K_1(\tilde{\omega}r_0)-I_1(\tilde{\omega}r_0)K_1(\tilde{\omega}R)}-cr. \tag{33}$$

Inserting $d(r)$ back into Eq. (32) allows us to calculate F_{dh} and from that to obtain the inclusion-induced relative change of the membrane's bending stiffness for spherical deformation, κ_{rel}, as defined in Eq. (16). The final result is

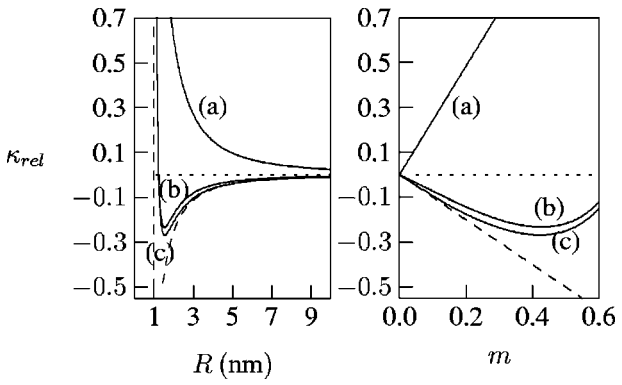

FIG. 8. The inclusion-induced relative change in stiffness of the membrane segment, $\kappa_{\rm rel}$, according to Eq. (34), plotted as a function of R (left graph) and $m=r_0^2/R^2$ (right graph) for (a) $\omega=20/\text{nm}$, (b) $\omega=2/\text{nm}$, (c) $\omega=0.2/\text{nm}$. The remaining parameters are $\eta=1$, $r_0=1$ nm, and $\bar{\alpha}=0$. The broken line displays the limiting case for $\tilde{\omega}=0$, namely, $\kappa_{\rm rel}=-1/(1+\rho)=-m$. Note that the parameters in curves (a)–(c) of the two graphs correspond to those in Fig. 5.

$$\kappa_{\rm rel}=\frac{1}{1+\rho}\left[\frac{1}{\tilde{P}(1+\eta^2)(1+\bar{\alpha})}-1\right], \tag{34}$$

where the function

$$\tilde{P}=\frac{2}{\tilde{\omega}r_0}\frac{I_1(\tilde{\omega}R)K_1(\tilde{\omega}r_0)-I_1(\tilde{\omega}r_0)K_1(\tilde{\omega}R)}{I_1(\tilde{\omega}R)K_0(\tilde{\omega}r_0)+I_0(\tilde{\omega}r_0)K_1(\tilde{\omega}R)} \tag{35}$$

is the same as in Eq. (17), yet with ω replaced by $\tilde{\omega}$. It is interesting to note that in the limit $\kappa_h\to\infty$ it is $\omega=\tilde{\omega}$ and thus $P=\tilde{P}$; but even in that limit $\kappa_{\rm rel}$ in Eq. (34) remains different from Eqs. (20) [for which we recall $\kappa_{\rm rel}(\eta\to\infty)=-1$]. Thus, the case of uniform local curvature of the cell [Fig. 1(b)] is not contained in Eq. (20) as a special case.

Let us analyze Eq. (34). In the limit of vanishing tilt modulus ($\kappa_t=0$), the membrane can adjust to the shape of the inclusion through a tilt deformation without an energetic penalty. In this case, we have $\tilde{\omega}=0$ or, equivalently, $\tilde{P}\to\infty$. Equation (34) then predicts $\kappa_{\rm rel}=-1/(1+\rho)=-(r_0/R)^2=-m$, which corresponds to a reduction of the bending stiffness by the area fraction the inclusions occupy in the membrane. This result is plausible because a fraction of $m=(r_0/R)^2$ lipids is eliminated from participating in the curvature deformation, and there is no additional interaction between the inclusion and the membrane.

In the opposite limit, that of infinitely large tilt modulus, the membrane can no longer adjust its shape during bending to that of the inclusion. Indeed, $\kappa_t\to\infty$ (or, equivalently $\tilde{\omega}\to\infty$) implies $\tilde{P}=0$ and thus $\kappa_{\rm rel}\to\infty$.

Figure 8 shows $\kappa_{\rm rel}$ as a function of R (left graph) and $m=(r_0/R)^2$ (right graph) for the same parameters as Fig. 5. Note that a major feature, i.e., the possibility to locally soften the membrane ($\kappa_{\rm rel}<0$) is also present for suppressed relaxation of the membrane shape. On the other hand, in the limit of large tilt modulus, local membrane softening is absent for both constrained and unconstrained local membrane perturbations. The main difference between the unconstrained [Fig. 1(a)] and the constrained [Fig. 1(b)] local microscopic perturbations of the membrane shape around the intercalated inclusion is the different lower bounds, $\kappa_{\rm rel}=-1$ and $\kappa_{\rm rel}=-m$, respectively, the former being adopted for $\eta=\kappa_h/\kappa_s\to\infty$ and the latter for $\tilde{\omega}=\kappa_t/\kappa_s=0$. Hence, the magnitude of the local membrane softening can, in principle, be more pronounced in the case of unconstrained membrane shape perturbations around the inclusion [Fig. 1(a)].

F. Relation to phenomenological interaction constants and intrinsic curvatures of single-inclusion energy

Expressing F_{dh} as an expansion with respect to $c_1=c_2=c=H$ [Eq. (14)] allows us to estimate the phenomenological parameters $2K+\bar{K}$ and H_m, describing the single inclusion energy [Eq. (1)] of an isotropic inclusion ($D_m=0$) in a spherical membrane curvature field ($H=c$ and $D=0$),

$$E_i=\mu_m+(2K+\bar{K})(c-H_m)^2, \tag{36}$$

where the curvature c is defined at the mesoscopic level. For both restricted and unrestricted microscopic perturbations of the membrane shape around the isotropic (and rigid) inclusion, comparison of Eqs. (14) and (36) yields

$$2K+\bar{K}\simeq\frac{\pi}{2}R^2\kappa_0\kappa_{\rm rel}, \tag{37}$$

$$H_m\simeq\frac{(1+\kappa_{\rm rel})}{\kappa_{\rm rel}}c_0. \tag{38}$$

Recall that the energy of a single inclusion, E_i in Eq. (1), is assumed not to depend on the inclusion density m. Hence, also $2K+\bar{K}$ should be independent of m. According to Eq. (37) (or, equivalently, $\kappa_{\rm rel}=2m(2K+\bar{K})/\pi r_0^2\kappa_0$), this is the case as long as $\kappa_{\rm rel}\sim m$. Indeed, this relation is fulfilled for a wide range of parameters, both for restricted and unrestricted local microscopic membrane shape perturbations, as can be seen in Figs. 5 and 8. In fact, it is always fulfilled in the small m regime apart from the case $\kappa_t\to 0$ for unrestricted membrane shape relaxation (corresponding to the lower broken line in Fig. 5). This allows us to calculate $2K+\bar{K}$ via a small m expansion of $\kappa_{\rm rel}$. Specifically, in the limit of vanishing Gaussian modulus, $\bar{\kappa}=0$, we deduce from Eq. (22) for unconstrained local membrane shape relaxation

$$2K+\bar{K}=\frac{\pi r_0^2\kappa_0}{2}\left[1-\frac{2\eta^2}{\omega r_0}\frac{K_1(\omega r_0)}{K_0(\omega r_0)}\right], \tag{39}$$

whereas the case of constrained local membrane shape relaxation yields according to Eq. (34)

$$2K+\bar{K}=\frac{\pi r_0^2\kappa_0}{2}\left[-1+\frac{\tilde{\omega}r_0}{2(1+\eta^2)}\frac{K_0(\tilde{\omega}r_0)}{K_1(\tilde{\omega}r_0)}\right]. \tag{40}$$

Note that vanishing of $2K+\bar{K}$ in Eq. (39) is consistent with the condition for $\kappa_{\rm rel}=0$ in Eq. (28).

For a typical choice of material parameters [corresponding to curve (b) in Fig. 5], the relation $\kappa_{\rm rel}\sim m$ holds up to $m\approx 0.2$ for unrestricted membrane shape relaxation. Note

also that, as expected, $\kappa_{\mathrm{rel}} \sim m$ is not fulfilled for large m where the (long-range) lipid deformations around neighboring inclusions overlap.

In the case of restricted microscopic perturbation of the membrane shape around the rigid inclusion [Fig. 1(b)], the decay of lipid (tilt) perturbation around the membrane inclusion is exponential (i.e., short range). Therefore, the overlapping of the short-range lipid deformations around neighboring inclusions becomes important only if the inclusions are very close. Consequently K, $\bar{K}$, and H_m depend on the local density of the inclusions only for very large m.

III. DISCUSSION AND CONCLUSIONS

For a bare lipid membrane (in absence of rigid inclusions), spherelike bending leads to uniform curvature everywhere. That is, all lipids in each of the two membrane leaflets are perturbed in the same way, and they all contribute to the corresponding bending stiffness. If inclusions are present within the membrane with a certain area fraction $m=r_0^2/R^2$, the number of lipids that contribute to the deformation energy per unit area is reduced by a fraction $m=1/(1+\rho)$. If, hypothetically, the remaining lipids would not experience any additional perturbation due to the inclusions (and thus would remain with uniform local spherelike curvature $c_1=c_2=c$ and no tilt deformation everywhere), the corresponding bending stiffness would be $\kappa_{\mathrm{rel}}=-m$ which indeed appeared as a special case in Sec. II E for $\kappa_t=0$ [see Eq. (34), and the discussion thereafter]. The corresponding mechanism of this hypothetical case is obvious: previously perturbed lipids do no longer contribute to the deformation energy (per unit area) once they are replaced by rigid inclusions. To approach a more realistic scenario, the structural perturbation of the membrane by rigid inclusions and the ability of the lipids to locally adjust at a microscopic level should be accounted for.

Consider first the structural perturbation of a small membrane segment by the inclusions while still retaining locally uniform spherelike mesoscopic curvature; $c_1=c_2=c$ everywhere in the segment. This scenario was subject of Sec. II E. Here, the membrane must adjust to the shape of the inclusion through a tilt deformation [Fig. 1(b)]. This deformation is short range and can thus be translated into a (positive) line tension along the inclusion rim, or, equivalently, into a (positive) inclusion-membrane interaction energy. Whether inclusions locally soften or rigidify the membrane segment then depends on the magnitude of this interaction energy. The two terms in Eq. (34) reflect the two opposite tendencies: local membrane rigidification due to the interaction term and the $-m$ softening contribution. We note that the assumption of the unperturbed local membrane shape around the membrane-embedded inclusion [Fig. 1(b)] forms the basis for a number of recent investigations [41,42] and allows one to estimate the inclusion-membrane interaction energy also for *anisotropic* inclusions.

Consider now the influence of adding the degree of freedom to adjust the local membrane shape at the microscopic level [Fig. 1(a)]. This was the subject in Sec. II B. Here again, the general result for κ_{rel}, Eq. (20) [and similarly the limit for $\bar{\alpha}=0$ in Eq. (22)], appears as a sum of two competing terms, favoring rigidification and softening. Yet, here the competition cannot be straightforwardly interpreted in terms of a line tension (or, equivalently, in terms of a membrane-inclusion interaction energy). In fact, the concept of a membrane-inclusion interaction energy independent of the inclusion density is not generally valid because the curvature-induced inclusion-inclusion interactions are long range. The most notable consequence of the long-range nature is that already very small inclusion densities can, in principle, lead to dramatic local membrane softening. This can happen for $\kappa_t=0$ and $\bar{\kappa}=0$. To this end, compare the small m limit of κ_{rel} in Eq. (24), namely, $\kappa_{\mathrm{rel}}=-\eta^2/(1+\eta^2)+m$, to the corresponding expression for locally prescribed, uniform spherelike, curvatures, $\kappa_{\mathrm{rel}}=-m$ (displayed as the lower broken lines in the right graphs of Figs. 5 and 8). The mechanism for the local softening at already small inclusion densities m lies in maintaining a catenoidlike membrane shape; that is, adopting the long-range membrane shape $h(r)=cR^2\ln(R/r)$ for any imposed spherelike curvature c at the cell boundary R. Maintaining such a catenoidlike saddle shape is favorable as it does, given that $\bar{\kappa}=0$, not infer a bending penalty. At the same time, it can only be maintained for variable curvature c if a vanishingly small tilt modulus ($\kappa_t=0$) decouples the membrane shape from the cone angle imposed by the inclusion. Indeed, the corresponding membrane shape $h(r)=cR^2\ln(R/r)$ is independent of the inclusion structure (of size r_0 and cone angle d_0).

Despite the differences in the two approaches—unconstrained or constrained local microscopic membrane shape perturbation (Fig. 1)—both predict the possibility of local membrane softening. This is in contrast to eliminating the lipid tilt degree of freedom ($\kappa_t \to \infty$) for which inclusions always stiffen the host membrane [see Eq. (30) or (31)]. Hence, our major conclusion is that the lipid tilt degree of freedom plays a significant role for the energetics of inclusion-containing lipid membrane patches.

A notable result is the nontrivial influence of the Gaussian modulus on the effective bending stiffness, κ_{rel}, of a spherical membrane segment. The Gaussian modulus $\bar{\kappa}$ can usually be ignored for topologically invariant membranes because of the Gauss-Bonnet theorem. This is also the case in the presence of inclusions, if the inclusions are rigid and if the membrane energetics is dominated entirely by bending energy. Yet, the last requirement is not fulfilled in the present study because of the additional tilt degree of freedom. Mathematically, the dependence on $\bar{\kappa}$ (or, equivalently, on $\bar{\alpha}$) enters through the second boundary condition of Eqs. (12), which specifies optimization of $h(r)$ at the inclusion rim $r=r_0$. Only in the limit $\kappa_t \to \infty$ does the dependence $\kappa_{\mathrm{rel}}=\kappa_{\mathrm{rel}}(\bar{\alpha})$ reduce to a simple prefactor $1/(1+\bar{\alpha})$; see Eq. (30). In this trivial case, the only appearance of the Gaussian modulus in κ is as an additive contribution $4\bar{\kappa}$; see Eq. (31). In the general case, for finite κ_t, the Gaussian modulus enters into κ in a nontrivial way, but generally acts effectively toward local rigidification of the membrane.

The present work employs a number of approximations. One is the cell model, which disregards correlations and the true multibody nature of the membrane-mediated interac-

tions between inclusions. Similar cell models are nevertheless a common method to describe inclusion-containing membranes [9,10]. Another assumption is the presence of a reservoir of lipid molecules (i.e., the presence of an extended, stress relaxed lipid bilayer). Taking into account a fixed number of lipids can be accomplished through an additional constraint, which, however, was not in the scope of the present work. In addition, for closed vesicle shapes, the nonlocal bending stiffness [Eq. (2)] and the area stretching of the lipid bilayer [19,45] may be important. The first adds to the overall elastic free energy F_{dh} a term proportional to $k_n(\int \Delta h da)^2/\int da$, where the value for the nonlocal bending rigidity k_n is for lipid bilayers expected to be of the order of the (local) bending rigidity [46]. The second contribution, due to relative area change, adds to F_{dh} a term proportional to $K_s(\int \Delta h^2 da)^2/\int da$. Although this is a fourth-order contribution, the area compressibility modulus K_s is quite large for lipid bilayers ($K_s \approx 0.2$ J/m$^2 \approx 50$ kT/nm^2 [50]). Therefore, if the inclusions occupy a significant portion of the overall membrane area, both "global" terms should be taken into account for closed membrane shapes. As already mentioned in the Introduction, at larger total number of membrane-embedded inclusions (N), the nonlocal bending energy term restricts the local microscopic perturbation of the membrane shape around the intercalated inclusion (Fig. 1) [see also Eq. (3)].

In the present work, we also adopt the assumption of uniform lateral distribution of the membrane inclusions. Abandoning this assumption would add an additional degree of freedom to the system that would allow inclusions to accumulate at regions of favorable curvatures and in this way decrease the membrane bending constants [37,38,43].

In the presented model, we also did not account for a spontaneous curvature of the "bare" lipid membrane. Hence, if there are no inclusions present, a flat membrane is the optimal free energy state and, as discussed at Eq. (15), this implies for an inclusion-free membrane that $c_0=0$. However, we may introduce the spontaneous curvature of a lipid bilayer by changing the first and the third term in Eq. (7) to $\kappa_s(\nabla\cdot\mathbf{d}-c_0^{(s)})^2$ and $\kappa_h(\Delta h-c_0^{(h)})^2$. Here, the constant terms $c_0^{(s)}$ and $c_0^{(h)}$ represent a spontaneous splay and a bare spontaneous curvature. Note that the new constant terms contribute to the free energy only terms linear in $\nabla\cdot\mathbf{d}$ and Δh, and thus do not affect the bending stiffness of a lipid membrane. The spontaneous curvature, on the other hand, changes. An inclusion-free membrane now has the spontaneous curvature $c_0=-2(\kappa_s c_0^{(s)}+\kappa_h c_0^{(h)})/\kappa_0$. Also for the inclusion-containing membrane, the corresponding calculation can be carried out. The result is especially simple in the case of $c_0^{(s)}=c_0^{(h)}$ and for vanishing Gaussian modulus, where the spontaneous curvature depends linearly on the cone angle, radius, and density of the membrane inclusions, namely, $c_0=-md_0/r_0-(1-m)c_0^{(s)}/2$.

From a biological perspective, a possible application of our model of unrestricted membrane shape perturbation around the inclusion [Fig. 1(a)] is accumulation and mutual interaction of coat proteins during the process of local membrane budding [49]. Here, a local membrane softening induced by more rigid membrane constituents could possibly facilitate the bud formation.

A possible application of our model for the case of restricted local membrane shape perturbation around the membrane inclusions [Fig. 1(b)] can be the membrane budding during the crenation of erythrocyte membrane [39]. In erythrocytes, the budding takes place over the whole cell membrane surface (although is located predominately at the top of membrane spicules) [34]. Because of that, the membrane shape perturbation around the membrane inclusions are strongly restricted [see Eq. (3)]. Therefore, the local membrane softening in the budding region due to accumulation of the membrane proteins [39] is a consequence of the change of tilt of lipid molecules around the proteins only [Fig. 1(b)] and not of the microscopic membrane shape perturbation [Fig. 1(a)].

To summarize this work, we have shown that isotropic conelike membrane-embedded rigid inclusions can locally soften a lipid bilayer membrane. The crucial quantity responsible for this ability is the lipid tilt degree of freedom. We also argued that the constrained microscopic membrane shape perturbation around the intercalated rigid inclusion [Fig. 1(b)] still allows for local membrane softening whereas ignoring the lipid tilt degree of freedom invariably leads to local membrane stiffening.

ACKNOWLEDGMENTS

We wish to acknowledge the support of ARRS of the RS (Grants No. P2-0232-1538 and No. BI-US/05-06/014). S.M. acknowledges financial support from ND EPSCoR through National Science Foundation Grant No. EPS-0132289.

[1] H. Gruler, Z. Naturforsch. C **30c**, 608 (1975).
[2] S. Marčelja, Biochim. Biophys. Acta **367**, 165 (1974).
[3] S. Marčelja, Biochim. Biophys. Acta **455**, 1 (1976).
[4] D. R. Fattal and A. Ben-Shaul, Biophys. J. **65**, 1795 (1993).
[5] T. Gil, J. H. Ipsen, O. G. Mouritsen, M. C. Sabra, M. M. Sperotto, and M. J. Zuckermann, Biochim. Biophys. Acta **1376**, 245 (1998).
[6] M. Goulian, Curr. Opin. Colloid Interface Sci. **1**, 358 (1996).
[7] S. May, Curr. Opin. Colloid Interface Sci. **5**, 244 (2000).
[8] N. Dan, P. Pincus, and S. A. Safran, Langmuir **9**, 2768 (1993).
[9] H. Aranda-Espinoza, A. Berman, N. Dan, P. Pincus, and S. A. Safran, Biophys. J. **71**, 648 (1996).
[10] C. Nielsen, M. Goulian, and O. S. Andersen, Biophys. J. **74**, 1966 (1998).
[11] M. Goulian, R. Bruinsma, and P. Pincus, Europhys. Lett. **22**, 145 (1993).
[12] M. Kardar and R. Golestanian, Rev. Mod. Phys. **71**, 1233 (1999).
[13] T. R. Weikl, M. M. Kozlov, and W. Helfrich, Phys. Rev. E **57**, 6988 (1998).

[14] T. Chou, K. S. Kim, and G. Oster, Biophys. J. **80**, 1075 (2001).
[15] K. S. Kim, J. Neu, and G. Oster, Biophys. J. **75**, 2274 (1998).
[16] P. G. Dommersnes and J. B. Fournier, Eur. Phys. J. B **12**, 9 (1999).
[17] V. Kralj-Iglič, V. Heinrich, S. Svetina, and B. Žekš, Eur. Phys. J. B **10**, 5 (1999).
[18] P. G. Dommersnes and J. B. Fournier, Biophys. J. **83**, 2898 (2002).
[19] W. Helfrich, Z. Naturforsch. C **28**, 693 (1973).
[20] M. Hamm and M. M. Kozlov, Eur. Phys. J. E **3**, 323 (2000).
[21] J. B. Fournier, Eur. Phys. J. B **11**, 261 (1999).
[22] W. Helfrich and J. Prost, Phys. Rev. A **38**, 3065 (1988).
[23] Y. Kozlovsky and M. M. Kozlov, Biophys. J. **82**, 882 (2002).
[24] M. Rappolt, A. Hickel, F. Bringezu, and K. Lohner, Biophys. J. **84**, 3111 (2003).
[25] M. Hamm and M. M. Kozlov, Eur. Phys. J. B **6**, 519 (1998).
[26] S. May and A. Ben-Shaul, Biophys. J. **76**, 751 (1999).
[27] T. C. Lubensky and F. C. MacKintosh, Phys. Rev. Lett. **71**, 1565 (1993).
[28] J. B. Fournier, Europhys. Lett. **43**, 725 (1998).
[29] U. Seifert, J. Shillcock, and P. Nelson, Phys. Rev. Lett. **77**, 5237 (1996).
[30] S. May, Eur. Biophys. J. **29**, 17 (2000b).
[31] V. Markin, Biophys. J. **36**, 1 (1981).
[32] U. Seifert, Adv. Phys. **46**, 13 (1997).
[33] M. Laradji and P. B. Sunil Kumar, Phys. Rev. Lett. **93**, 198105 (2004).
[34] V. Kralj-Iglič, H. Hägerstrand, P. Veranič, K. Jezernik, D. R. Gauger, and A. Iglič, Eur. Biophys. J. **43**, 1066 (2005).
[35] J. M. Allain and M. B. Amar, Physica A **337**, 531 (2004).
[36] U. Seifert, Phys. Rev. Lett. **70**, 1335 (1993).
[37] S. Leibler, J. Phys. (Paris) **47**, 507 (1986).
[38] V. Kralj-Iglič, S. Svetina, and B. Zekš, Eur. Biophys. J. **24**, 311 (1996).
[39] H. Hägerstrand, L. Mrowczynska, U. Salzer, R. Prohaska, K. Michelsen, V. Kralj-Iglič, and A. Iglič, Mol. Membr Biol. **23**, 277 (2006).
[40] V. Kralj-Iglič, M. Remškar, G. Vidmar, and A. Iglič, Phys. Lett. A **296**, 151 (2002).
[41] M. Fošnarič, K. Bohinc, D. R. Gauger, V. Kralj-Iglič, A. Iglič, and S. May, J. Chem. Inf. Model. **45**, 1652 (2005).
[42] J. B. Fournier, Phys. Rev. Lett. **76**, 4436 (1996).
[43] B. Božič, V. Kralj-Iglič, and S. Svetina, Phys. Rev. E **73**, 041915 (2006).
[44] W. Helfrich, Z. Naturforsch. C **29c**, 510 (1974).
[45] E. A. Evans and R. Skalak, *Mechanics and Thermodynamics of Biomembranes* (CRC Press, Boca Raton, 1980).
[46] W. C. Hwang and R. E. Waugh, Biophys. J. **72**, 2669 (1997).
[47] S. May, Y. Kozlovsky, A. Ben-Shaul, and M. M. Kozlov, Eur. Phys. J. E **14**, 299 (2004).
[48] D. P. Siegel and M. M. Kozlov, Biophys. J. **87**, 366 (2004).
[49] J. Zimmerberg and M. M. Kozlov, Nat. Rev. Mol. Cell Biol. **7**, 9 (2006).
[50] G. Cevc and D. Marsh, *Phospholipid Bilayers: Physical Principles and Models* (Wiley, New York, 1987).